Multidisciplinary Optimisation of Flexible Aircraft Structures in Consideration of Flight Control System Demands in the Time Domain

Daniel Nussbächer[1(✉)], Ögmundur Petersson[1], Fernass Daoud[1], and Mirko Hornung[2]

[1] Airbus Defence and Space GmbH, Rechliner Str., 85077 Manching, Germany
daniel.nussbaecher@airbus.com
[2] Technische Universität München, Boltzmannstr. 15, 85748 Garching, Germany

Abstract. Today's industrial optimisation process for aircraft structures does not consider flight control systems. In this paper a method to couple flight control systems with aerostructural design in the scope of optimisation is presented. Further, an overview on necessary methodical enhancements coming with controller integration is given. The integration is demonstrated on a flexible aircraft model. A generic pitch controller is coupled with the aeroelastic solver. It is demonstrated how a simple disturbance of a trimmed state can be controlled and how critical time steps can be detected. Wing skin composite layers are sized with the selected loads. Structural responses from the controlled system are compared to those of the uncontrolled system for both the baseline and the optimised model.

Keywords: Aeroservoelasticity · Aircraft structural sizing

1 Introduction

In modern aircraft industry the dimensions of structural components can be sized using multidisciplinary design optimisation (MDO) in consideration of aeroelastic but not flight control system (FCS) related demands. For highly flexible aircraft, the loads commanded by a respective flight control system and resulting from aero-structural coupling effects affect the final design. Main bottleneck is that in the state of the art structural optimisation process, transient effects are considered by means of pre-calculated static load cases, only. The consideration of transient controller effects during optimisation runs, means a potential reduction of final control design complexity. Current research in the field of aeroservoelasticity mainly is subjected to analysis capabilities. A good overview on the basics of aeroservoelasticity without further discussions on industrial optimisation is given by Tewari in [1]. Karpel et al. apply a simple controller to a gust

H. C. Rodrigues et al. (Eds.): *EngOpt 2018 Proceedings of the 6th International Conference on Engineering Optimization*, pp. 1385–1397, 2019.
https://doi.org/10.1007/978-3-319-97773-7_119

load case in [2]. In [3] design optimisation considering aeroservoelastic demands is presented by Haghighat et al. for aircraft wing structures, using beam modelling. Wildschek et al. present an integrated control and optimisation method working on wing beam and shell models in [4]. Important discussions on aspects of unsteady aerodynamic methods is given by Kier in [5]. Structural notch filter optimisation is demonstrated for a combat aircraft by Luber in [6]. This paper focusses on structural optimisation of composite materials for full scale industrial models under consideration of both aeroelastic and control system demands. For this purpose the optimisation capabilities of the Airbus in-house MDO tool LAGRANGE are extended and applied for a representative use case. The aeroelastic analysis, used for structural optimisations, is enhanced by an interface for flight control systems and is further coupled to a dynamic structural solver.

2 Components of Classical Aircraft Structural Optimisation in Consideration of Aeroelasticity

Before enhancing the current aircraft structural sizing process, a general understanding of its main ingredients must given. The two main components can be identified as the mathematical formulation of the optimisation problem itself, and the system equations of the underlying analysis.

2.1 Mathematical Formulation of the Optimisation Problem

In general, a mathematical optimisation problem is formulated such that an objective function f is to be optimised (minimised or maximised) while certain inequality or equality constraint functions g or h shall meet pre-given conditions by variation of a set of design variables x, which need to be selected from feasible ranges given by respective lower and upper limits $x_{i,l}$ and $x_{i,u}$:

$$\min_{\mathbf{x}} \left\{ f(\mathbf{x}) \middle| \mathbf{g(x)} \geq 0, \mathbf{h(x)} = 0, \forall x_i \in [x_{i,l}, x_{i,u}] \right\} \tag{1}$$

Equation (1) is formulated as a minimisation problem. It shall be noted, that inequality constraints g are formulated such that a design is considered to be feasible for positive values of the constraint function ($g(x) \geq 0$), in this paper. The classical engineering optimisation problem in aeronautic applications aims to reduce aircraft mass, while assuring structural integrity by variation of structure related variables. Structural integrity is achieved when stressing variables as mechanical strain or stress values (ϵ and σ) remain under allowable values, which depend on the chosen material and a respective failure criterion. Physical variables as cross sectional areas, sheet thicknesses, ply angles and ply thicknesses for composite materials are grouped into sets of design variables x in order to study the effect of how changing their values affect the structural response of a given system:

$$\min_{x} \left\{ m(x) \middle| \epsilon \leq \epsilon_{all}, x_l \leq x \leq x_u \right\} \tag{2}$$

In practical applications the objective and constraint functions, and the design variables will be standardised in Eq. (2), before handing them to a numerical optimiser.

2.2 Equations of Aeroelasticity

For the applications in this paper, the physical base for an optimisation of aircraft structures is given in the governing equations of aeroelasticity. The key point there is the interconnection between structural mechanics and aerodynamics. The interaction between the mechanical and the aerodynamic model is mainly represented by the bi-directional exchange of aerodynamic loads and the induced structural displacements. A deformed structure affects the resulting loads, and the resulting loads again affect the resulting structural deformation, see Fig. 1.

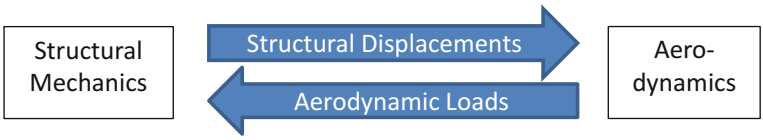

Fig. 1. Aeroelastic interconnection

In this paper, the interconnection is summarised in the aeroelastic equations of motion, based on the work of Rodden and Love [8]:

$$(K - qQ) \cdot u + M \cdot \ddot{u} = qQ_x \cdot u_x + P \tag{3}$$

where

- K and M are the structural stiffness and mass matrices
- q is the dynamic pressure
- Q and Q_x are aerodynamic stiffness matrices
- u and $\ddot{u}$ are the structural displacements and accelerations
- P is the additional external loading
- u_x are aerodynamic degrees of freedom

The aerodynamic stiffness matrices Q and Q_x result from aerodynamic forces being transferred into the structural domain using the infinite plate spline theory [9]. Aerodynamic degrees of freedom in u_x are mainly angles of attack and control surface deflections. Rigid body motions of a free flying, unclamped structure are considered by an inertia relief approach and represented through the accelerations $\ddot{u}$.

3 Coupled Analysis of Aerostructural Dynamics and Control System

A critical step to the consideration of control system inputs in the optimisation process is to couple a controller to the aeroelastic analysis. Therefore, basics on general control system design need to be discussed. Hereafter, the physical interface to aeroelasticity is explained.

3.1 Basics on Control System Modelling

Control systems can be used when a dynamic system shall maintain a given or reach a desired state. One task of a flight controller is to improve the dynamics of eigenmodes and rigid body movements. This is mainly achieved by actively damping the respective modes through control parameters [10]. The dynamic system to be controlled is referred to as "plant" G. "Open loop" control means commanding inputs u_c for a specific plant without receiving feedback on how the command changed the plant behaviour. When feeding back outputs y of the plant to generate inputs for the controller C, a "closed loop" control system is generated, see Fig. 2. The plant output is compared with a pre-defined, desired output w ("setpoint") which results in a control error e forwarded as controller input. The controller thus monitors the plant and is enabled to actively manipulate its dynamic behaviour.

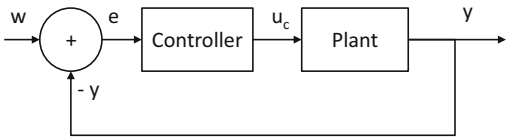

Fig. 2. Closed loop control

From the system modelling point of view it can be noted:

– The control error $e(t)$ w.r.t. the a dynamic setpoint $w(t)$ states as

$$e(t) = w(t) - y(t) \tag{4}$$

– The controller C is a time-dependent function with $e(t)$ being the function input and the control command $u_c(t)$ being the function output:

$$C : e(t) \rightarrow u_c(t) \tag{5}$$

– The plant G is a time-dependent function with $u_c(t)$ being the function input and the system response $y(t)$ being the function-output:

$$G : u_c(t) \rightarrow y(t) \tag{6}$$

Of main importance is to quickly reach and maintain a small control error. To measure the quality of a controller for a given task, the integrated absolute error IAE is suggested:

$$IAE = \int_0^T |e(t)|dt \tag{7}$$

Considering the absolute value of e over the time interval to study ($t \in [0, T]$) prevents that positive and negative parts in e cancel each other out. IAE can be used to compare different control systems: The smaller IAE, the better the control task is fulfilled.

3.2 Controlling Components of Aeroelasticity

Main variables in flight control are the aircraft elevator deflections η for the longitudinal axis and the aircraft ailerons and rudder ξ and ζ for the lateral axis [10]. For aircraft systems, the general commands described in Sect. 3.1 are control surface commands η_c, ξ_c and ζ_c, which are forwarded to an actuation system, initiating the respective physical control surface deflections. From the methodical point of view the control surface deflections represent the interface between flight controller and aeroelastic analysis. The command is applied as an input to the aeroelastic analysis by means of u_x in Eq. (3) and therefore results in an aerostructural deformation resulting from the initiated aeroelastic loading:

$$P_{el} + P_{ad} + P_{rbm} = P_x + P_{ext} \tag{8}$$

with

- the elastic load component $P_{el} = K \cdot u$
- the splined aerodynamic load component $P_{ad} = -qQ \cdot u$
- the rigid body mode load component $P_{rbm} = M \cdot \ddot{u}$
- the additional aerodynamic load component $P_x = qQ_x \cdot u_x$
- additional, external load component P_{ext}

The primary effect of a control surface deflection can be seen in a change in P_{rbm}, which leads to a rigid body mode acceleration. From the structural dynamics point of view, both the elastification given with P_{el} and the rigid body mode acceleration given with P_{rbm} can be considered by a respective solver, already. Therefore the remaining aeroelastic components in Eq. (8) hold a special meaning w.r.t. a dynamic solution:

$$P_{ext,d} = -P_{ad} + P_x + P_{ext} \tag{9}$$

The dynamic structural solution in this paper is provided by a generalized alpha method [7]. It solves the general system equation

$$M \cdot \ddot{u} + D \cdot \dot{u} + K \cdot u = P_{ext,d} \tag{10}$$

The aerostructural load components, presented in Eq. (9) are now forwarded as externally applied loads $P_{ext,d}$ for each time step of the generalised alpha solver. A critical component here, is the damping matrix D. The Rayleigh damping model which simply states D to be a linear combination of stiffness and mass matrix K and M, shall be given as an example to capture damping effects in the system:

$$D = \alpha_1 M + \alpha_2 K \tag{11}$$

The dynamic solution provides elastic deformations u, velocities $v = \dot{u}$ and accelerations $a = \dot{v}$. This set of system responses provides variables which are fed back as controller inputs after comparison with the respective set value w. For rate control, rotational velocities are selected as variables to be controlled. The approach presented to couple the different analyses is summarised by the process flow in Fig. 3.

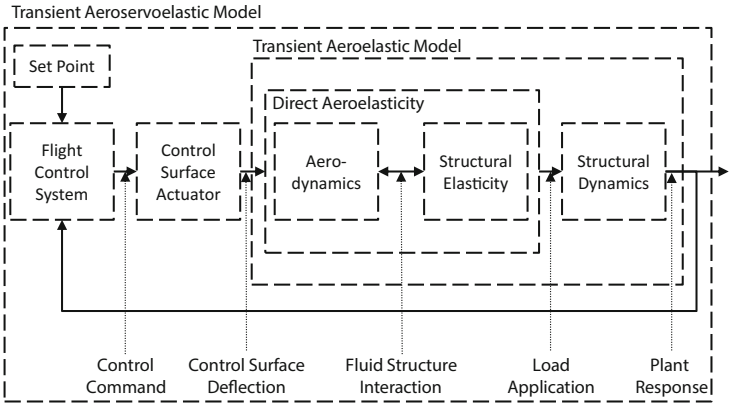

Fig. 3. Process flow of transient aeroservoelastic analysis

4 Respecting Control System Commands in the Optimisation Process

The introduction of a FCS increases the amount of data generated through the analysis step. It therefore necessitates a method to detect and select structurally critical time steps in order to reduce numerical costs.

Detection of Structurally Critical Time Steps. For a model with n structural constraints g_i and m time steps, the total number of constraints for optimisation was $n \cdot m$. LAGRANGE provides an enveloping tool that gathers all constraints in a matrix g_{ij} ($i \in [1, n]$ and $j \in [1, m]$). The most critical time steps are subsequently selected based on the lowest constraint values. As a result, loads for those time steps along with the affected elements (see Fig. 4) are stored externally such that they can directly be used in a following optimisation run.

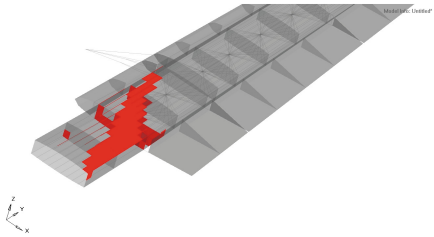

Fig. 4. Detecting structurally critical elements

Data and Process Flow. With the capability to detect critical time steps and respective critical structural components from the coupled analysis sizing optimisation tasks using controlled loads can now be solved. The resulting optimised design must critically be re-analysed and studied. Design modifications often lead to significant changes in the system behaviour, not expected beforehand. The sequential process is shown in Fig. 5.

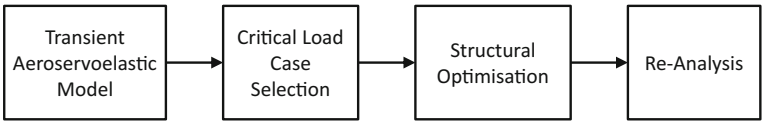

Fig. 5. Current optimisation process using a transient aeroservoelastic analysis

5 Application to a Highly Elastic Aircraft Configuration

In the following, an aircraft configuration will be presented which is mainly designed by aeroelastic effects. It is therefore a good example to demonstrate the application of a rate control mechanism in system analysis and the interconnection of aeroelasticity and control system in industrial optimisation.

5.1 The OptiMALE Aircraft Model

The aircraft model being studied is a medium altitude long endurance (MALE) configuration called "OptiMALE". The finite element model consists of approximately 31.000 structural grid-points, which results in 186.000 structural degrees of freedom. Both aluminium and composite materials are considered for the structural components. The main elements being studied in this paper are wing skin elements, which are all made out of composite material with varying numbers of layers. The OptiMALE is a very flexible configuration with a structural mass of $8.5t$ and a span from tip to tip of approximately $28m$. The aerodynamic model is based on the doublet lattice method [11]. The aerodynamic surfaces are discretised into 2800 aerodynamic boxes. For the fluid structure interaction the

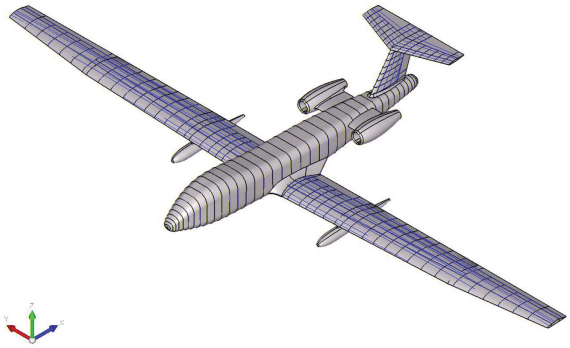

Fig. 6. The OptiMALE aircraft model

infinite plate spline theory is applied [9]. The flight state being studied in this paper is given by a mach-number of 0.4 and an altitude of $10.000m$. A geometric representation of the OptiMALE structural model can be seen in Fig. 6.

5.2 Disturbance and Control

The use case to demonstrate optimisation with an aeroservoelastic analysis, represents the OptiMALE being disturbed by an external load from its originally trimmed, steady state. The tasks are to improve the dynamics of re-gaining the steady state by application of a simple pitch controller and to reduce mass by structural optimisation. The OptiMALE is trimmed, using Eq. (3). The resulting state is used as initial condition in a structural dynamic calculation. As an artificial, external disturbance, a distributed load is applied for the time range of $[3s, 3.7s]$ resulting in a pitch. The amount of this disturbance is 40% of the structural weight.

Side note: The area of validity for the aerodynamic model is limited. For high angles of attack, the doublet lattice approach can not be considered as valid any more. Further, the assumption of quasi-steady states was made in the aeroelastic solution. Therefore a data base, generated from runs with high-fidelity aerodynamic tools, was consulted through the runs to detect violations of these assumptions.

A simple pitch controller is now applied to reduce the energy from the elastic oscillations resulting from the disturbance. The pitch controller is tracking the pitch rate $q_k(t)$ (rotational velocity about y-axis) of the aircraft. As a response to an undesired pitch rate, the controller commands an elevator deflection $\eta(t)$, such that a counteracting pitch moment is applied to the aircraft. The control task is to maintain the pitch rate $q_k(t)$ at a setpoint value of $q_{SP} \stackrel{!}{=} 0$:

$$e(t) = q_{SP} - q_k(t) \tag{12}$$

The pitch control system is given as a time-discrete proportional-integral-derivative (PID-) controller. The gains k_p, k_i, k_d were design w.r.t. a satisfactory IAE-value:

$$u_c(t) = k_p e(t) + k_i \int_0^t e(\tau) d\tau + k_d \dot{e}(t) \tag{13}$$

Figure 7 shows the dynamic system responses when no controller is applied. In the strain plots, the strain values are normalised w.r.t. the peaks of the uncontrolled system. Figure 8 shows the system responses with the selected controller in the loop.

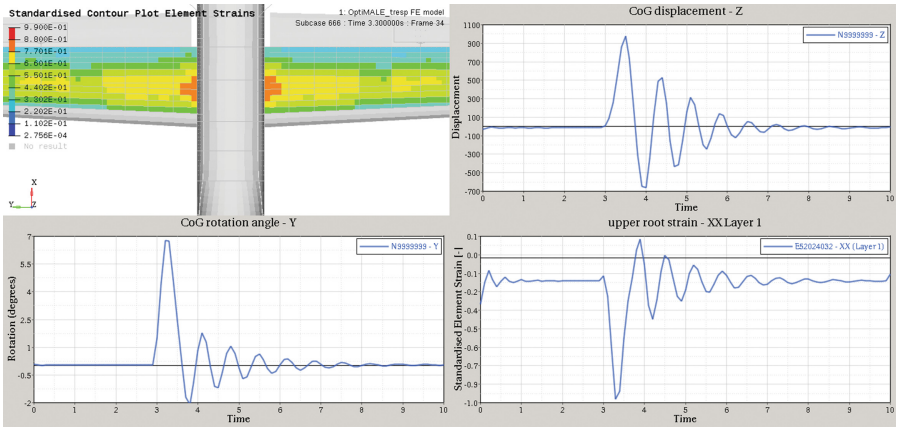

Fig. 7. Responses of the uncontrolled aeroelastic system

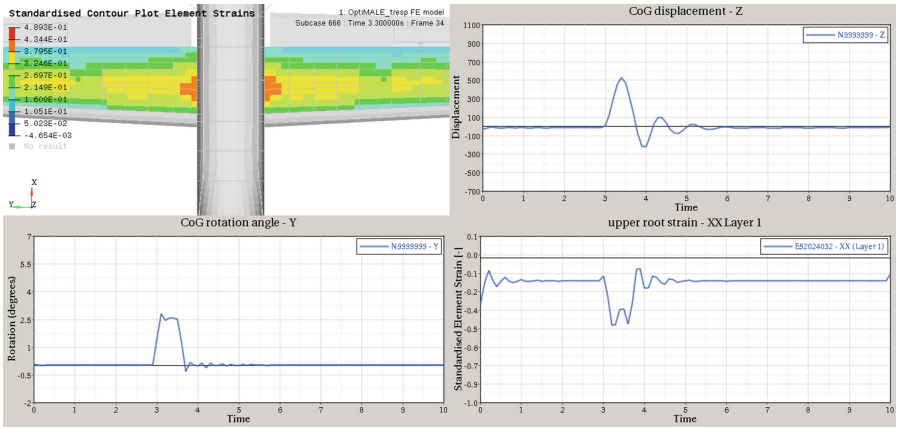

Fig. 8. Responses of the controlled aeroelastic system

5.3 The Engineering Optimisation Problem

With the given pitch controller and the resulting controlled loads, composite layers in the wing of the OptiMALE shall be sized. According to Eqs. (1) and (2), the optimisation problem physically states as follows:

- Objective function f: Overall structural mass
- Design variables x: Approx. 600 design variables grouping ply thickness values in composite elements, distributed over the aircraft wings
- Constraint functions g: Strain values in up to 40 layers of 5110 composite elements close to the wing root section are constrained according to their maximum allowable values.

It must be noted that the potential mass saving is limited, as only wing composite elements shall be varied. Mass affected by the selected design variables is 4% of the overall mass, only. The optimisation procedure selected to solve this task is a classical sequential linear programming (SLP) algorithm.

5.4 Structural Optimisation Results

First, the wing composites are sized for the open loop response. From the optimisation run in Fig. 9 it can be seen, that the final mass is achieved after few optimisation iterations. The maximum constraint violation and the number of active constraints, show that the optimiser has significant problems in converging to a design. The constant change in constraints while maintaining the structural mass after few iterations can be explained by a thickness-increase of composite layers in the root area and a reduction in the tip area of the wing. From a physical point of view this is a plausible result as the main bending moment acts in the wing root area, where the structure must thus be stiffened the most. The responses of the re-analysed system is depicted in Fig. 10.

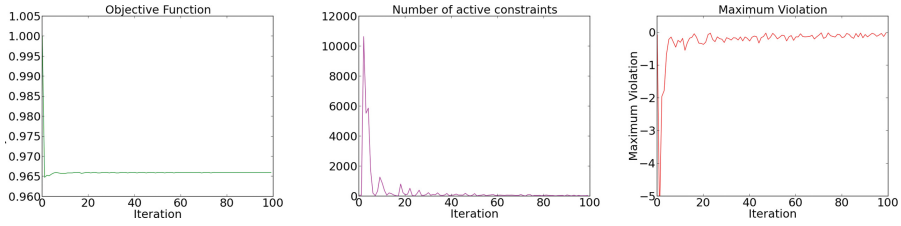

Fig. 9. Objective function, number of active constraints and maximum constraint violation over the optimisation run without active controller

In the second run, the closed loop response is used for sizing the wing composite layers. With loads manipulated by the control system, the optimisation runs become smoother, as can be seen in Fig. 11. This is mainly due to the fact

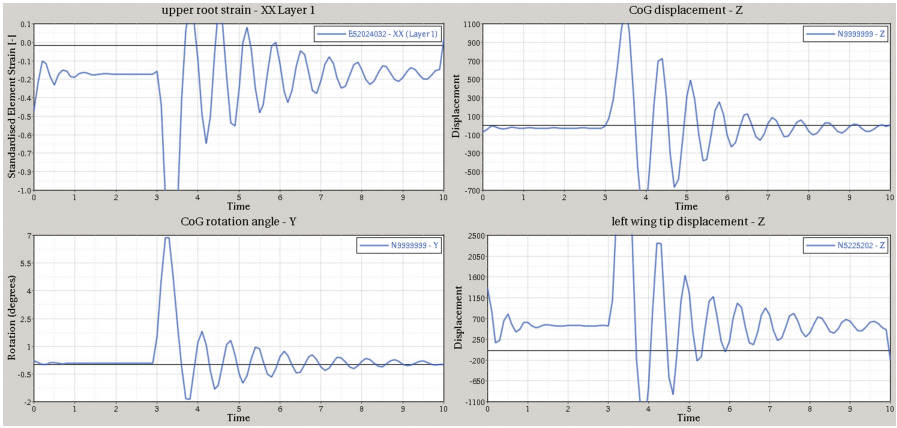

Fig. 10. Response of the optimised system without active controller

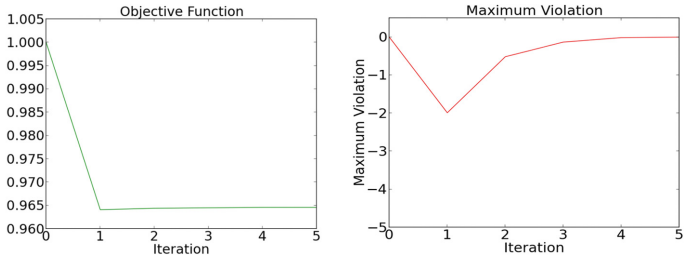

Fig. 11. Objective function, number of active constraints and maximum constraint violation over the optimisation run with active controller

that the structure does not experience the same amount of stressing input as without the control system. The secondary effect of load reduction by application of the simple controller can be studied by comparing the strain components in Figs. 7 and 8. A reduction of approximately 50% can be spotted. This positively affects the optimisation runs, as the optimiser finds a feasible design within few iterations. Figure 12 depicts the response of the optimised system with active controller.

For both re-analyses, the experienced strains of the optimised system are higher, compared to the original ones. This is an expected result as during the optimisation layer thicknesses in the composite elements are reduced for the purpose of mass reduction. With less material to carry the external load, the resulting internal strains increase.

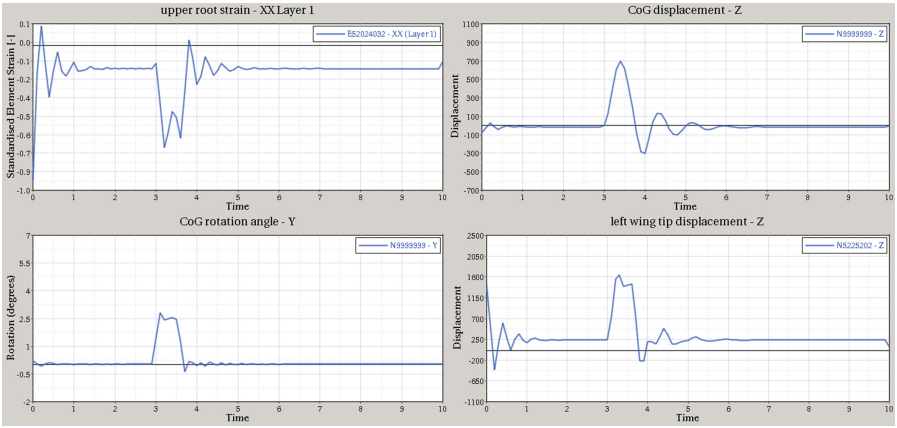

Fig. 12. Response of the optimised system with active controller

6 Conclusion

This paper presented a method to couple flight control systems to the industrial MDO process. An overview on aeroelastic components from the current optimisation process was given. Load components from the aeroelastic equations of motion were used to manipulate the solution process of structural dynamics. For this purpose FCS commands were applied as control surface deflections to the aeroelastic solver. It was presented how the resulting aeroservoelastic system responses may be filtered and serve as a base for engineering optimisation tasks. The resulting aeroservoelastic process was demonstrated at a generic MALE aircraft configuration disturbed from a levelled flight. It can be summarised that the consideration of flight control laws in MDO tasks reduces the loads experienced by the structure and helps to find better aircraft designs.

References

1. Tewari, A.: Aeroservoelasticity - Modeling and Control. Springer-Verlag, New York (2015). https://doi.org/10.1007/978-1-4939-2368-7
2. Karpel, M., Moulin, B., Chen, P.C.: Dynamic response of aeroservoelastic systems to gust excitation. J. Aircr. **42**(5), 1264–1272 (2005). https://doi.org/10.2514/1.6678
3. Haghighat, S., Martins, J.R.R.A., Liu, H.H.T.: Aeroservoelastic design optimization of a flexible wing. J. Aircr. **49**(2), 432–443 (2012). https://doi.org/10.2514/1.C031344
4. Wildschek, A., Pranante, B., Kanakis, T., Tongeren, H.V., Huls, R.: Concurrent optimization of a feed-forward gust loads controller and minimization of wing box structural mass on an aircraft with active winglets. In: 16th AIAA/ISSMO Multidisciplinary Analysis and Optimization Conference, AIAA AVIATION Forum, (AIAA 2015-2490) (2015). https://doi.org/10.2514/6.2015-2490

5. Kier, T.: An integrated loads analysis model including unsteady aerodynamic effects for position and attitude dependent gust fields. In: 15th International Forum on Aeroelasticity and Structural Dynamics (2011). https://elib.dlr.de/73763
6. Luber, W.: Aeroservoelastic flight control design for a military combat aircraft weapon system. In: 28th Congress of the International Council of the Aeronautical Sciences, Brisbane, Australia (2012)
7. Chung, J., Hulbert, G.: A time integration algorithm for structural dynamics with improved numerical dissipation: the generalized-α method. J. Appl. Mech. **60**(2), 371–375 (1993). https://doi.org/10.1115/1.2900803
8. Rodden, W.P., Love, J.R.: Equations of motion of a quasisteady flight vehicle utilizing restrained static aeroelastic characteristics. J. Aircr. **22**(9), 802–809 (1984). https://doi.org/10.2514/3.45205
9. Harder, R.L., Desmarais, R.N.: Interpolation using surface splines. J. Aircr. **9**(2), 189–191 (1972). https://doi.org/10.2514/3.44330
10. Brockhaus, R., Alles, W., Luckner, R.: Flugregelung. Springer-Verlag, Heidelberg (2011). https://doi.org/10.1007/978-3-642-01443-7
11. Albano, E., Rodden, W.P.: A doublet-lattice method for calculating lift distributions on oscillating surfaces in subsonic flows. AIAA J. **7**(2), 279–285 (1969). https://doi.org/10.2514/3.5086